Supplementary Information

Crystallization of Methylammonium Lead Halide Perovskites by Optical Trapping

Ken-ichi Yuyama,[a],* Md Jahidul Islam,[a] Kiyonori Takahashi,[a] Takayoshi Nakamura,[a] and Vasudevanpillai Biju[a],*

[a]Research Institute for Electronic Science, Hokkaido University, Kita 20 Nishi 10, North Ward, Sapporo, Hokkaido 001-0020, Japan

Table of Contents

1. Experimental procedure

We used the following chemicals without any further purification; MACl (TCI, >98.0%), MABr (TCI, >98.0%), MAI (TCI, >98.0%), $PbCl_2$ (Aldrich, 98.0%), $PbBr_2$ (Aldrich, ≥98.0%), PbI_2 (Aldrich, 99.0%), dimethyl sulfoxide (DMSO) (Wako), *N,N*-dimethylformamide (DMF) (Wako), and γ-butyrolactone (GBL) (TCI, >99.0%). Precursor solutions of $MAPbBr_3$ and $MAPbI_3$ were prepared by mixing equimolar precursors in DMF and GBL, respectively, and the mixture was stirred at 1000 rpm for 1 hr. In the case of $MAPbCl_3$, a precursor solution was prepared by dissolving equimolar precursors in DMSO, which was followed by the addition of DMF to the solution. These sample solutions were centrifuged at 10000 rpm for 5 min, and their supernatants were filtered through a nanopore membrane (220 nm) before optical trapping experiments. The sample chamber was fabricated by gluing a silicone rubber O-ring to a cover glass (Matsunami, 25 mm×25 mm, thickness 0.13–0.17 mm) using silicone glue (ShinEtsu, KE42RTV). The diameter and height of the chamber are 4 mm and 3 mm, respectively. A thin layer (100–200 μm) of a precursor solution was prepared by placing ca 10 μL of it into the handmade sample chamber.

The optical system was constructed based on an inverted microscope (Olympus, IX71). A continuous-wave laser beam of 800 nm (Coherent Mira 900) or 1064 nm (Spectron Laser System) was used as the light source in optical trapping. The laser was focused onto the solution surface with an objective lens of 60 times magnification (Olympus, UPlanFLN, numerical aperture; 0.90). The laser power was measured after beam was passed through the objective lens. The sample set on the microscope stage was illuminated with white light from a halogen lamp and observed with a commercial imaging camera (Watec, WAT250D). The sample chamber was heated from above with a thermoplate (TOKAI HIT, TP-110R-100) as necessary. Following

trapping, the temperature of the plate is set at 90 ^{o}C during the crystal growth. During the crystal growth, we observed the crystal with a low magnification (×10 or ×4) objective lens. In laser trapping experiments, the laser power was varied from 100 to 600 mW and precursor concentrations were varied from 0.1 M to 1.3 M. From these parameters, we identified the threshold power for trapping induced crystallization at 200 mW. Also, the minimum concentration of precursor solution is 1.2 M.

After single crystal was grown up to 400×400 μm^2 or larger in the solution of MACl/$PbCl_2$ or MABr/$PbBr_2$, we picked the crystal from the sample chamber and analyzed the structure of the crystal by single crystal X-ray diffraction (XRD) method. The crystal was mounted on the glass capillary and fixed with epoxy resin. Crystallographic data were collected using a Rigaku RAXIS-RAPID diffractometer with Mo-Kα (λ = 0.71073 Å) radiation from a graphite monochromator. Structural refinements were performed using the full-matrix least-squares method on F^2. The calculations were carried out with Yadokari-XG software package.[1,2] Powder XRD patterns were constructed with Mercury software[3] based on the resultant CIF files from the analyses. Experimental details are available in SI as CIF files.

2. Optical trapping-induced crystallization of $MAPbCl_3$ and $MAPbI_3$ with 1064 nm laser

As the samples for optical trapping, we used MACl/$PbCl_2$ (1.0 M) dissolved in DMSO:DMF solvent mixture (1:1, v:v) and MAI/PbI_2 (1.0 M) dissolved in GBL. $MAPbCl_3$ show retrograde solubility in a DMSO:DMF (1:1, v:v) mixture at temperatures up to 100 °C.[4] In the case of $MAPbI_3$ in GBL, the solubility increases with temperature up to 60 °C, but retrograde solubility is observed at 60–120 °C.[5] Based on these solubility details, the saturation degrees of respective solutions were estimated at 0.85 and 1.2, which is at 18 °C in the experimental room.

Figure S1a shows optical trapping behavior upon the 1064 nm laser irradiation into the solution surface of MACl/$PbCl_2$. A small crystal of a few micrometers was identified in a camera image at 93 s. The nucleated crystal grew large while being trapped at the focal spot. The growth was saturated with the crystal size ca 5×5 μm^2. For further growth of the crystal, we heated the sample chamber with a thermoplate, which was after the nucleation [panel (ⅰ) of Fig.S1b]. The nucleated single crystal grew continuously under the combined trapping and heating condition. After the crystal size became ca 60 × 60 μm^2, the trapping laser was turned off, and the crystal continued to grow under heating, which was observed through a low magnification objective lens [panels (ⅱ)-(ⅲ) of Fig. S1b]. The XRD data (Fig. S1c) obtained for the grown single crystal perfectly match with the characteristic pattern of cubic form of $MAPbCl_3$.[4]

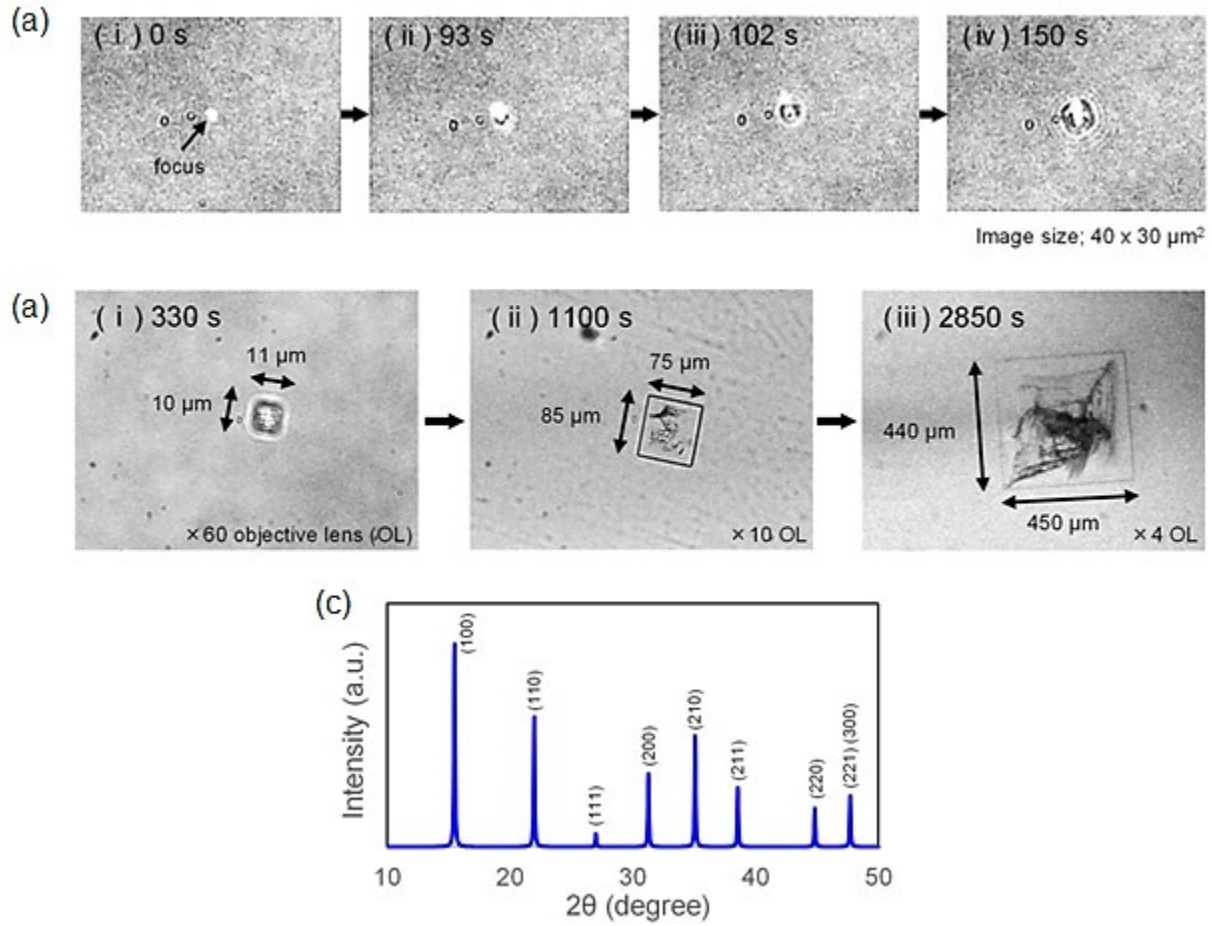

Fig. S1| a) Optical micrographs in the solution of $MACl/PbCl_2$ under the 1064 nm laser irradiation at the solution surface. The laser power throughout the objective lens is 0.6 W. b) Optical micrographs of the crystal that was incubated in the chamber heated with a thermo-plate set at 90 ℃. The dark spots outside the crystal are from dust in the microscope optics, whereas those in the crystal are due to inhomogeneous thickness of the crystal. The dark sports c) The calculated powder XRD pattern of the large crystal formed by optical trapping.

Apart from the solutions of $MACl/PbCl_2$ and $MABr/PbBr_2$, we didn't observe any crystallization in a solution of MAI/PbI_2 exposed to the trapping laser for 30 min at room temperature. Interestingly, crystallization was induced under optical trapping in a MAI/PbI_2 solution set at 100 ℃with a thermoplate. Suddenly, many black crystallites were formed at the focal spot [panels (i)–(ii) of Fig. S2], and the

number of crystals was increased within 1 to 2 seconds [panel (iii) of Fig. S2]. Followed by the formation, the crystals were detached from the focal spot [panel (iv) of S2] and dissolved while moved away to the surrounding solution. We could not characterize the formed crystals, because they dissolved soon after the detachment from the focal spot or the trapping laser was turned off. By considering the black color of $MAPbI_3$ perovskite crystal, we suggest that the microcrystals formed in a MAI/PbI_2 solution under optical trapping should be $MAPbI_3$. At room temperature, the solubility of $MAPbI_3$ is increased with temperature elevation. Therefore, immediately after the formation of a $MAPbI_3$ crystallite at the focal spot, it might have dissolved through the efficient two-photon induced heating. On the other hand, $MAPbI_3$ has retrograde solubility under the heated condition, leading to explosive crystal growth through the rapid elevation of saturation degree.

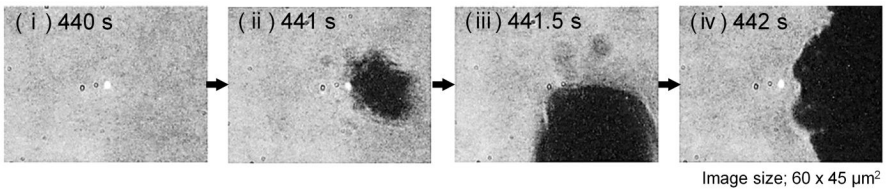

Fig. S2| Optical micrographs in the solution of MAI/PbI_2 under the 1064 nm laser irradiation at the solution surface. The laser power throughout the objective lens is 1.0 W.

3. Estimation of local temperature elevation during optical trapping with the use of 1064 and 800 nm laser

To estimate local temperature elevation, we refer to the paper reported by Miyasaka *et al.*[6] The local temperature elevation during optical trapping with the power of 1 W (ΔT (K)) is

proportional to α/λ (WK^{-1}), where α and λ are the absorption coefficient at the wavelength of the trapping laser and thermal conductivity, respectively. The slope between ΔT and α/λ is 0.75. Nonetheless, ref. 6 does not correlate laser trapping at the liquid-vapor interface. Furthermore, local temperature elevation in optical trapping at the air/solution surface remain undisclosed.

Absorption coefficients of 3 solvents used were determined by measuring their transmittance at 1064 and 800 nm passing through a glass cuvette with different optical path length, which was carried out using a spectrophotometer (Thermo Fisher Scientific Inc., Evolution 220). Figure S3A-C shows transmittance of each solvent at 1064 and 800 nm passing through a glass cuvette with optical path length of 1 to 5 cm. In the case of 800 nm, the transmittance was almost constant due to low light absorption. On the other hand, the transmittance of 1064 nm light decreased exponentially with the increase in the path length in accordance with the Beer-Lambert's law. From the fitting of an exponential function, we obtained extinction coefficients, which are summarized in table S1.

In order to discuss the impact of solutes on laser heating, we estimated absorption coefficients of the representative precursor solution ($MAPbBr_3$ in DMF). Fig. S3D shows transmittance of 800 and 1064 nm light passing through a $MAPbBr_3$ precursor solution. The absorption coefficients at respective wavelengths were less than 0.1 m^{-1} and 1.36. At 800 nm, light absorption is negligibly small, and local temperature elevation can be ignored during the laser irradiation. Extinction spectra are shown in Fig. S3E. At 1064 nm, the absorption coefficient is low compared to that of pure DMF. This result indicates that the absorption of 1064 nm light becomes week with the increase in the concentration of the precursors of $MAPbBr_3$. We speculate that a $MAPbBr_3$ crystal has an absorption coefficient in the level of 1 m^{-1} at 1064 nm. This estimation also supports that the contribution of solutes ($MAPbBr_3$

precursors) to the light absorption and accompanying heating is small compared to pure solvent (DMF).

In order to investigate the impact of two-photon absorption by the precursor solutions, we measured absorption spectra of respective precursor solutions in a cuvette of 1 mm optical path length (Fig. S3E). The reference spectrum was obtained for air. The $MAPbI_3$ precursor solution was diluted 100 times before the measurement. The $MAPbBr_3$ precursor solution has an absorption edge at 400 nm, so that laser heating through two-photon absorption of the precursor solution might partially contribute to the nucleation of $MAPbBr_3$ under the 800 nm laser irradiation. Since the $MAPbI_3$ precursor solution is expected to show strong two-photon absorption of the 800 nm, we did not carry out trapping experiments with 800 nm laser.

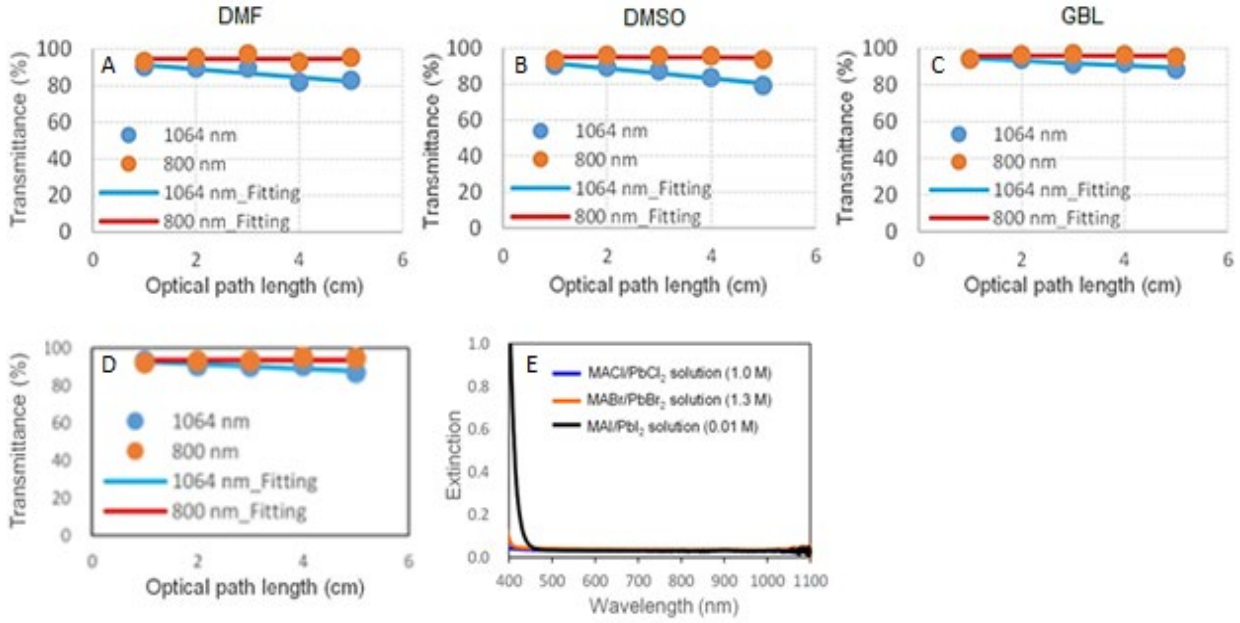

Fig. S3| A-C) Transmittance of the 1064 and 800 nm light passing through the solvents used in the present work as a function of path length. D) Transmittance of a $MAPbBr_3$ solution (50 mM) in DMF for different pathlengths. E) Extinction spectra of precursor solutions (0.1 to 1.3 M).

Thermal conductivities of respective solvents are reported in the literatures.[7–9] As summarized in table S1, local temperature elevation is negligibly small in the case of trapping using 800 nm laser. On the other hand, 1064 nm laser with the power of 1.0 W leads to temperature elevation by 10–13 K in pure solvents. DMSO and DMF have the similar dielectric and optical absorption properties, so that DMSO/DMF mixed solvent should show temperature elevation of 10–13 K/W. The local temperature elevation for $MACl/PbCl_2$ and $MABr/PbBr_2$ solutions is estimated at <8 K under the present 1064 nm laser irradiation condition. In the solution of MAI/PbI_2, the temperature elevation is estimated at 10 K, and its contribution to the change in saturation degree depends upon heating conditions of the sample chamber. Without the use of a thermoplate, the local temperature elevation lowers the saturation degree. When the sample is heated with the thermoplate, laser-induced heating elevates the saturation degree, which is due to the retrograde solubility of MAI/PbI_2.

	Absorption coefficient (m^{-1})		Thermal conductivity (W/m·K)	Temperature elevation coefficient $\Delta T/\Delta P$ (K/W)	
	1064 nm	800 nm		1064 nm	800 nm
DMF	2.62	< 0.1	0.183	10.7	< 0.5
DMSO	3.22		0.186	13.0	
GBL	1.42		0.100	10.6	

Table S1| Absorption coefficients, thermal conductivities, and local temperature elevation for solvents of perovskite precursors.

4. Optical trapping-induced crystallization of $MAPbCl_3$ and $MAPbBr_3$ with 800 nm laser

To suppress temperature elevation during the focused 1064 nm laser irradiation, we carried out the trapping experiments using 800 nm laser with the power of 0.4 W. As described above, temperature elevation under the 800 nm laser irradiation is negligibly small due to poor absorption of the laser. The trapping experiments were mostly carried out for $MACl/PbCl_2$ and $MABr/PbBr_2$, but not for the MAI/PbI_2 solution because of its strong two-photon absorption and temperature elevation. Figure S4a shows the trapping behavior upon the 800 nm laser irradiation at the surface of a $MACl/PbCl_2$ solution. The crystallization was induced from the focal spot at 210 s [panel (ii) of Fig. S4a]. The crystal grew slowly while being stably trapped at the focal spot, and the growth was saturated with the crystal size of 15 × 15 μm^2 [panels (iii)–(iv) of Fig. S4a]. Although the precursor solution doesn't absorb the trapping laser, the trapped crystal showed blue emission through two-photon absorption of the trapping laser (Fig. S4b). From the spectral profile, we consider the trapping-induced formation of a $MAPbCl_3$ crystal.

In the case of a solution of $MABr/PbBr_2$ under the 800 nm laser irradiation, the crystallization occurred at the focal spot (Fig. S4c). The size and the number of crystals were increased all at a sudden. Followed by the formation, the crystals were detached from the focal spot and moved away to the surrounding solution. This crystallization behavior is similar to the crystallization of $MAPbI_3$ with 1064 nm laser, which can be explained from the viewpoint of efficient two-photon induced heating and subsequent increase in saturation degree in the surrounding solution. During the nucleation and growth of the crystals, green emission was observed at the focal spot, which is the result of two photon absorption of the trapping laser by the $MAPbBr_3$ crystal. The peak position of emission spectra dynamically shifted around 540 nm (Fig. S4d). We assume that this fluctuation occurs due to factors such as rotation and breakage of

crystals and the crystal angle-dependent difference in the degree of reabsorption of emitted high energy photons.[7]

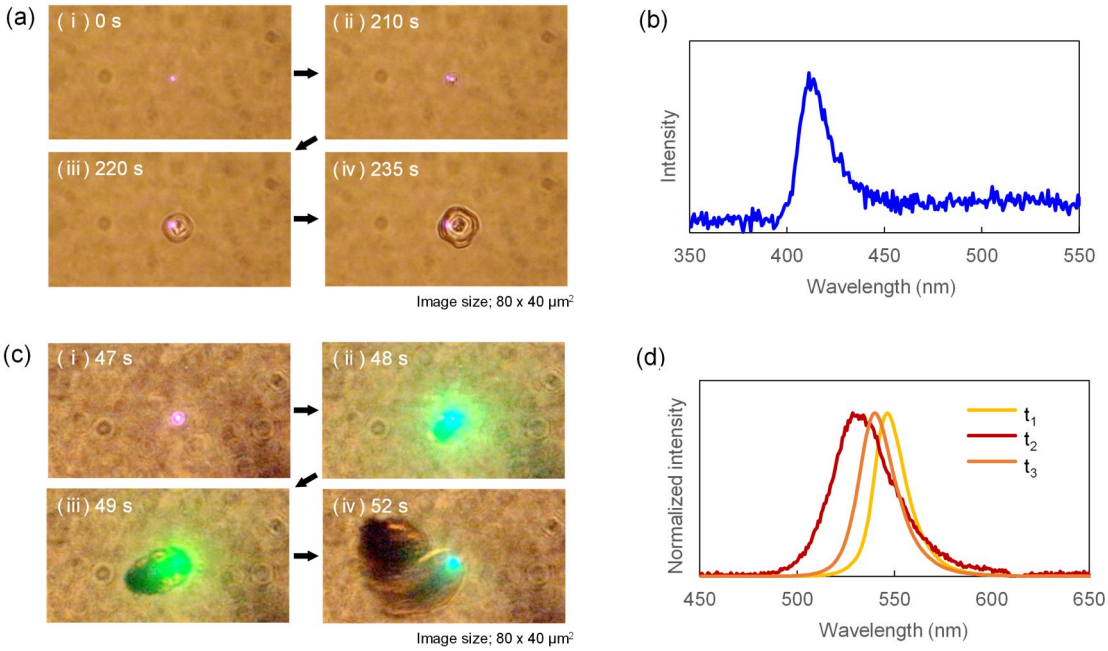

Fig. S4| Optical micrographs in the solutions of a) $MACl/PbCl_2$ and c) $MABr/PbBr_2$ under the 800 nm laser irradiation at the solution surface. The laser power throughout the objective lens is 0.4 W. Emission spectra of the crystals formed in the solutions b) $MACl/PbCl_2$ and d) $MABr/PbBr_2$ under the 800 nm laser irradiation. In d), t_1, t_2 and t_3 represent sequential spectra during trapping, showing spectral fluctuations.

5. Principle of optical trapping

The gradient force (***F***) exerted on nanometer-sized objects is given by

$$\boldsymbol{F} = \frac{1}{2}\varepsilon_m \alpha \nabla \boldsymbol{E}^2,$$

where $\boldsymbol{E}$ denotes the electric field, ε_m the dielectric constant of surrounding medium, ∇ the gradient with respect to the spatial coordinates, and α the polarizability of an object, which, under the dipole approximation, is given by

$$\alpha = 4\pi r^3 \frac{\left(\frac{n_p}{n_m}\right)^2 - 2}{\left(\frac{n_p}{n_m}\right)^2 + 2},$$

where notations r and n_p are the radius and the refractive index of the object, respectively, and n_m is the refractive index of the medium.

References

1. Yadokari-XG, Software for Crystal Structure Analyses, K. Wakita, (2001).

2. C. Kabuto, S. Akine, T. Nemoto, E. Kwon, Release of software (Yadokari-XG 2009) for crystal structure analyses. *J. Cryst. Soc. Jpn.* **51**, 218–224 (2009).

3. C. F. Macrae, I. J. Bruno, J. A. Chisholm, P. R. Edgington, P. McCabe, E. Pidcock, L. Rodriguez-Monge, R. Taylor, J. van de Streek, P. A. Wood, Mercury CSD 2.0 - New features for the visualization and investigation of crystal structures *J. Appl. Cryst.*, **41**, 466–470 (2008).

4. G. Maculan, A. D. Skeikh, A. L. Abdelhady, M. I. Saidaminov, M. A. Haque, B. Murali, E. Alarousu, O. F. Mohammed, T. Wu, O. M. Bakr, $CH_3NH_3PbCl_3$ single crystals: Inverse temperature crystallization and visible-blind UV-photodetector. *J. Phys. Chem. Lett.* **6**, 3781–3786 (2015).

5. M. I. Saidaminov, A. L. Abdelhady, G. Maculan, O. M. Bakr, Retrograde solubility of formamidinium and methylammonium lead halide perovskites enabling rapid single crystal growth. *Chem. Commun.* **51**, 17658–17661 (2015).

6. S. Ito, T. Sugiyama, N. Toitani, G. Kataya, H. Miyasaka, Application of fluorescence correlation spectroscopy to the measurement of local temperature in solutions under optical trapping condition. *J. Phys. Chem. B* **111**, 2365–2371 (2007).

7. *CRC Handbook of Chemistry and Physics, 96th Edition*; CRC Press, 2015.

8. J.-C. Zhou, Y.-Y, Che, K.-J. Wu, J. Shen, C.-H. He, Thermal conductivity of DMSO + C_2H_5OH, DMSO + H_2O, and DMSO + C_2H_5OH + H_2O mixtures at T = (278.15 to 338.15) K *J. Chem. Eng. Data* **58**, 663–670 (2013).

9. *Handbook of Thermal COnductivity, Volume 1, 1st Edition*; Gulf Professional Publishing, 1995.

10. H. Diab, C. Arnold, F. Lédée, G. Trippé-Allard, G. Delport, C. Vilar, F. Bretenaker, J. Barjon, J.-S. Lauret, E. Deleporte, D. Garrot, Impact of reabsorption on the emission spectra and recombination dynamics of hybrid perovskite single crystals *J. Phys. Chem. Lett.* **8**, 2977–2983 (2017).